Available online at www.sciencedirect.com
SCIENCE DIRECT®
Biomaterials 26 (2005) 1523–1532
Biomaterials
www.elsevier.com/locate/biomaterials

Fiber-based tissue-engineered scaffold for ligament replacement: design considerations and in vitro evaluation

James A. Cooper[a,b,c,d], Helen H. Lu[f], Frank K. Ko[e], Joseph W. Freeman[a], Cato T. Laurencin[a,b,c,d,*]

[a] Department of Orthopaedic Surgery, University of Virginia, 400 Ray C. Hunt Drive, Suite 330, Charlottesville, VA 22903, USA
[b] Department of Biomedical Engineering, University of Virginia, 400 Ray C. Hunt Drive, Suite 330, Charlottesville, VA 22903, USA
[c] Department of Chemical Engineering, University of Virginia, 400 Ray C. Hunt Drive, Suite 330, Charlottesville, VA 22903, USA
[d] Department of Biomedical Engineering, Drexel University, Philadelphia, PA 19104, USA
[e] Department of Materials Engineering, Drexel University, Philadelphia, PA 19104, USA
[f] Department of Biomedical Engineering, Columbia University, New York, NY 10027, USA

Received 15 April 2004; accepted 26 May 2004

Available online 17 July 2004

Abstract

The anterior cruciate ligament (ACL) is the major intraarticular ligamentous structure of the knee, which functions as a joint stabilizer. It is the most commonly injured ligament of the knee, with over 150,000 ACL surgeries performed annually in the United States. Due to limitations associated with current grafts for ACL reconstruction, there is a significant demand for alternative graft systems. We report here the development of a biodegradable, tissue-engineered ACL graft. Several design parameters including construct architecture, porosity, degradability, and cell source were examined. This graft system is based on polymeric fibers of polylactide-*co*-glycolide 10:90, and it was fabricated using a novel, three-dimensional braiding technology. The resultant microporous scaffold exhibited optimal pore diameters (175–233 μm) for ligament tissue ingrowth, and initial mechanical properties of the construct approximate those of the native ligament.

Keywords: Porosity; Degradable; Polymer; Anterior cruciate ligament; Ligament repair; Tissue engineering; Ligament and ligament tissue engineering

1. Introduction

The anterior cruciate ligament (ACL) is a commonly injured ligament of the knee, with over 250,000 patients each year diagnosed with a torn ACL, and approximately 150,000 ACL surgeries performed annually [1,2]. The ACL is an intraarticular ligament that controls normal motion and acts as a joint stabilizer. It connects the femur to the tibia and is completely enveloped by synovium. Due to the ACL's intrinsically poor healing potential and limited vascularization, ACL ruptures do not heal and surgical intervention is usually required. Current treatment modalities utilizing autogenous grafts such as bone–patellar tendon–bone and hamstring tendon have demonstrated clinically functional outcomes [3–9]. However, autogenous grafts are limited by donor site-related problems such as harvest site infection, nerve injury, and patellar fracture. Allografts are restricted in use due to the potential for infectious disease transfer and unreliable graft incorporation [10]. There are several commercially available synthetic ACL grafts, including the Gore Tex prosthesis, the Stryker–Dacron ligament, and the Kennedy ligament augmentation device (LAD) [5,11–13]. Although these synthetic grafts exhibit excellent short-term results, the long-term clinical outcome is poor due to mechanical mismatch, poor abrasion resistance, high incidence of fatigue failures, and limited integration between the graft and host tissue [14–17]. Clearly, alternative ACL replacement and reconstruction methods would be advantageous.

*Corresponding author. Department of Orthopaedic Surgery, The University of Virginia, 400 Ray C. Hunt Drive, Suite 330, Charlottesville, VA 22903, USA. Tel.: +1-434-243-0250.
E-mail address: ctl3f@virginia.edu (C.T. Laurencin).

0142-9612/$ - see front matter © 2004 Elsevier Ltd. All rights reserved.
doi:10.1016/j.biomaterials.2004.05.014

There is a growing interest in tissue-engineered solutions to musculoskeletal injuries. Tissue engineering may be defined as the application of biological, chemical, and engineering principles toward the repair, restoration, or regeneration of living tissues using biomaterials, cells, and factors alone or in combination [18]. The ideal ACL replacement scaffold should be biodegradable, porous, biocompatible, exhibit sufficient mechanical strength, and able to promote the formation of ligamentous tissue. Several groups have reported on potential ACL scaffolds using collagen, silk, biodegradable polymers, and composite materials [1,5,19–23]. Our approach to the design of functional ACL replacement grafts focuses on several parameters: architecture, porosity, degradability, and cell source. A strong emphasis is placed on understanding the effects of varying these three design parameters on the overall mechanical properties and cellular response to the tissue-engineered scaffold.

The architecture of the tissue-engineered scaffold is an important design consideration that can modulate biological response and long-term clinical success of the scaffold. It has been reported that calcified tissue ingrowth can occur at a minimum pore size of 100 μm [24]. In addition, a minimum pore diameter of 150 μm is suggested for bone and 200–250 μm for soft tissue ingrowth [11,25,26]. Scaffolds developed within these pore size ranges will encourage tissue ingrowth, capillary supply, and improve the quality of anchorage in bone tunnels. Overall scaffold porosity can modulate the functionality and gross cellular response to the implant. The presence of pore interconnectivity extending through an implant increases the overall surface area for cell attachment, which in turn can enhance the regenerative properties of the implant by allowing tissue ingrowth into the interior of the matrix.

The FDA has approved the use of the poly-α-hydroxyesters [polylactic acid (PLA), polyglycolic acid (PGA) and copolymers, polylactide-*co*-glycolide (PLAGA)] for a variety of clinical applications, and they have been investigated for use in tissue engineering [1,18,27–29]. The growing emphasis on the use of biodegradable materials is due to the fact that these materials do not elicit a permanent foreign body reaction, as they are gradually reabsorbed and replaced by natural tissue. In the long term, fatigue properties of the material may be less of a concern as the scaffold is eventually replaced by natural tissue. Therefore, PLAGA fibers, due to their well-documented biocompatibility, biodegradability, and extended clinical use as sutures and fixations devices, were chosen for study as part of a tissue-engineered scaffold.

The native ACL consists of a large number of fiber bundles arranged into three areas: anteromedial, posterolateral, and intermedial, accommodating low levels of friction tension during a wide range of motion [30,31]. By mimicking the collagen fiber matrix of the natural ACL, our approach was to engineer functional ACL scaffolds based on three-dimensional (3-D) fibrous hierarchical designs, utilizing novel braiding techniques which permit controlled fabrication of substrates with a desired pore diameter, porosity, mechanical properties, and geometry. The objective was to design a scaffold that would provide the newly regenerating tissue a temporary site for cell attachment, proliferation, and mechanical stability.

In addition to scaffold architecture and degradability, cell source and cellular response are also important consideration in ACL tissue engineering. Primary ACL fibroblasts derived from either explant or digestive cultures have a lower doubling rate compared to cells from other soft tissues. For in vitro culturing, rapid cell growth and maturation is desired in order to lower the wait time between cell harvesting and graft incorporation, which may be particularly important from a therapeutic standpoint. Therefore, other cell sources have been considered for ACL tissue engineering [32]. In this study, we performed an in vitro assessment of scaffold biocompatibility, where cell attachment, growth, and long-term matrix elaboration by primary ACL cells were compared to those of a murine fibroblast line. The primary criteria for cell selection were based on whether the alternative cell source can reproduce or mimic the response of native ACL cells when exposed to the designed replacement scaffold.

2. Materials and methods

2.1. Scaffold fabrication

The 3-D fibrous scaffolds were fabricated using customized, 3-D circular and rectangular braiding machines [33–35]. PLAGA 10:90 (Ethicon, NJ) fibers (52 deniers) were laced to produce yarns with a yarn density of 18 yarns per yarn bundle. The PLAGA yarns were then placed in a custom built circular braiding loom with a 3×16 carrier arrangement. The circular braiding machine uses the sequential motion of the carriers (alternating tracks) to form 48-yarn, 3-D circular braids with braiding angles that ranged from 26° to 31°. The scaffolds measured 2 cm in length for the porosity studies. For comparison in architecture and as an alternative design, the scaffolds were also fabricated using a 3-D rectangular braiding system in which PLAGA fibers were laced to produce yarns with yarn densities of 9, 30, and 60 yarns per bundle to investigate effects on mechanical and porosity parameters due to fiber number.

2.2. Scaffold characterization

The as-made scaffolds were characterized in terms of architecture (pore diameter, porosity, surface area), and

mechanical properties (tensile modulus, maximum tensile load) under tensile testing. These properties were correlated to fabrication parameters such as braiding angle and yarn density. The scaffold porosity needed for tissue ingrowth was measured for each braiding angle ($n = 3$) using a Micromeritics Autopore III porosimeter (Micromeritics, Norcross, GA). Changes in porosity, mode pore size, median pore size, and pore surface area were determined as a function of braiding angle for the 3-D scaffold. In addition, operator-dependent effects on scaffold porosity and pore diameter were examined using the 3-D rectangular braids. The mechanical properties of the braided 3-D PLAGA scaffolds ($n = 6$) under tension were evaluated using the Instron Testing System 1331 (Instron, MA) with a 2000 lb load cell. The gauge length was set at 1.03 cm and the sample tested at a speed of 0.020 cm/s (2%/s). The tensile modulus, ultimate tensile strength, and maximum tensile load were determined as a function of braiding angle.

2.3. Cells and cell culture

Primary ACL fibroblasts were isolated from 1 kg New Zealand White rabbits via enzymatic digestion following the methods of Amiel et al. [36]. Briefly, the ACL was excised from the rabbit knee under aseptic conditions, and the tissue was cut into small pieces and serial digested in a 0.1% collagenase solution (Sigma, St. Louis, MO). BALB/C CL7 mouse fibroblasts were purchased from American Type Culture Collection (ATCC, VA) and expanded in culture. Both cell types were cultured in α-MEM supplemented with 10% fetal bovine serum (FBS, Mediatech, Herndon, VA), L-glutamine and 1% antibiotics (Life Technologies, Invitrogen, CA), and maintained at 37°C and at 5% CO_2.

2.4. Scaffold in vitro evaluation

The response of ACL fibroblasts and a murine fibroblast cell line were examined on the braided 3-D scaffolds. Prior to cell seeding, the ACL scaffolds were exposed to UV light for 15 min on each side in an effort to minimize contamination [37]. The cells were seed on the scaffolds at a density of 400,000 cells/scaffold ($\sim$2900 cells/cm^2), and grown in supplemented α-MEM at 37°C and 5% CO_2. The cultures were maintained for up to 8 days. Cell growth and morphology were examined at 1 and 8 days using scanning electron microscopy (SEM). Prior to SEM analysis, the cells were fixed in glutaraldehyde, and dehydrated through a series of ethanol dilutions. The samples were sputter-coated with gold (Denton Desk-1 Sputter Coater, NJ). Cell growth and morphology were examined using an SEM system (Amray 3000, MA), at an accelerating voltage of 20 keV.

3. Results

3.1. Design of scaffold for ACL reconstruction

Our approach to the design of functional ACL replacement grafts focused on several parameters: architecture, porosity, degradability, and cell source. Specifically, the novel scaffold was based on a 3-D fibrous hierarchical design, utilizing novel braiding techniques which permitted controlled fabrication of substrates with a desired pore diameter, porosity, mechanical properties, and geometry. The objective was to design a scaffold that provides the newly regenerating tissue with a temporary site for cell attachment, proliferation, and mechanical stability. As shown in Fig. 1, the 3-D braided scaffold was comprised of three regions: femoral tunnel attachment site, ligament region, and tibial tunnel attachment site. The attachment sites had high angle fiber orientation at the bony attachment ends and lower angle fiber orientation in the intraarticular zone. This pre-designed heterogeneity in the grafts was aimed to promote the eventual integration of the graft with bone tissue. The scaffold was composed of PLAGA fiber with diameter similar to that of type I collagen fiber.

3.2. Scaffold porosity characterization

Results from the porosimetry analyses of the PLAGA circular and rectangular braided scaffolds are summarized in Table 1. The effects of braiding geometry on the linear density, mode pore diameter, median pore diameter, surface area, braiding angle, and porosity of the scaffolds can be derived from Table 1. All of the circular braids had the same number of yarns. Whereas the rectangular braids were tested with a different number of yarns per yarn bundle to observe changes in porosity of yarns with two different assistants combing the yarns to evaluate the consistency of the system. The mode pore diameter in Table 1 represents the average of the most frequent pore size of the pore size distribution of the scaffolds. The median pore diameter represents the pore size at which 50% of the pores are larger and 50% of the pores are smaller in the pore size distribution of the scaffolds. The surface area represents the total pore surface area within the scaffold and porosity represents a measure of the open spaces in the scaffold. The braiding angle represents the acute angle (as measured with SEM photomicrographs of the structure) that the yarn made with the vertical braid axis of the scaffold. Based on data shown in Table 1, it is evident that as the braiding angle increased from 26° to 31° for the circular braids that both the porosity and mode pore diameter significantly decreased, whereas the pore surface area significantly increased. The increase in total surface pore area with increasing

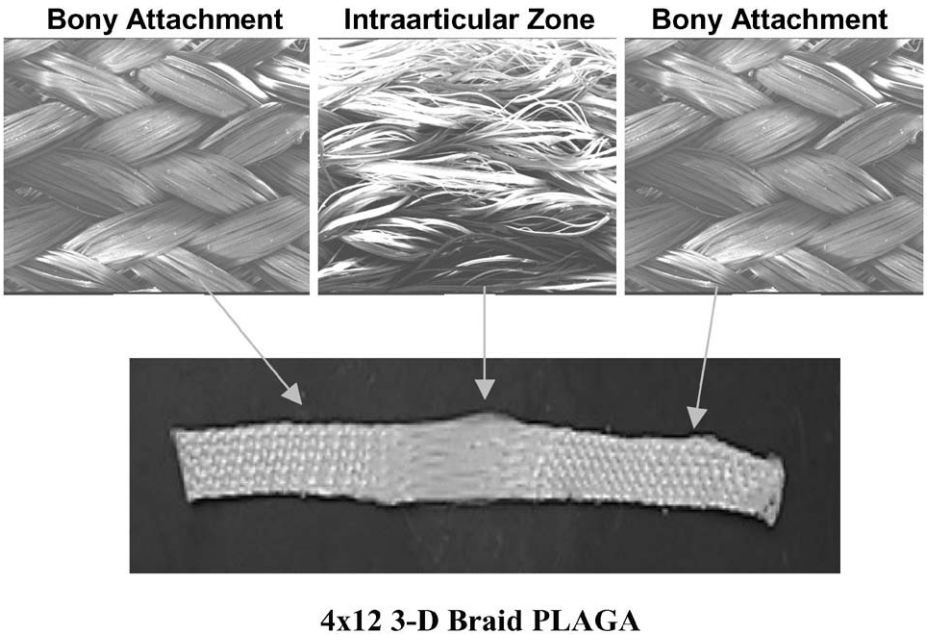

Fig. 1. General configuration of ligament scaffold design for 3-D rectangular braid.

Table 1
Summary of porosity data for 3-D circular and rectangular braids

Sample name	Sample number	Linear density (denier)	Mode pore diameter (μm)	Median pore diameter (μm)	Surface area (cm^2)	Braiding angle (deg)	Porosity (%)
Three-dimensional circular braid							
PLAGA (10:90) 3 × 16 (18 yarns)							
46 cm	4	52	233±19	136±16	135±5	26±3	63±2
36 cm	3	52	193±28	95±8	163±9	33±2	58±3
26 cm	3	52	175±35	79±4	165±5	31±1	54±1
Three-dimensional rectangular braid							
PLAGA (10:90) 5 × 12 (30 yarn)		52	195±35	84±6	71±35	27±6	55±5
PLAGA (10:90) 5 × 12 (60 yarn)	3	52	260±10	108±9	223±11	32±3	67±1
PLAGA (10:90) 4 × 12 Student 1 (9 yarns)	6	52	167±35	128±11	68±4	25±2	61±5
PLAGA (10:90) 4 × 12 Student 2 (9 yarns)	6	52	196±35	133±13	69±8	25±2	67±6

braiding angle was most likely due to the presence of higher numbers of pores with smaller pore size as evidenced by the decrease in mode pore diameter. An increase in total surface area was also found in the 3-D rectangular braids as yarns per bundle were increased from 30 to 60. In addition, the mode pore diameter, the median pore diameter, the braiding angle and porosity also increased with increased yarn bundle size. This was most likely due to the greater spaces created between the intertwined larger yarn bundles. When two different assistants combed the 3-D rectangular braids with the same number of yarns and the same braiding angle there was no change in any of the porosity data indicators.

3.3. Scaffold mechanical characterization

The mechanical properties (the maximum and ultimate tensile strength) of the scaffolds as a function of scaffold geometry, fiber number, and yarn density are summarized in Table 2. In addition, the effect of strain rate on the mechanical properties of the rectangular braid is shown in the same table. Fig. 2 demonstrates how braids composed of the same number and type of yarns differ in strength due to differences in strain rate and geometry. The initial maximum tensile loads were also investigated for 3-D circular braid. The scaffolds under tension exhibited a very short elastic region,

followed by a prolonged plastic deformation region. The scaffolds measured ultimate tensile strengths in the range of 100–400 MPa. The stress–strain profile was found to be similar to that of natural ligament tissue [30]. An example of the load–deformation curves of the 4×12, 3-D rectangular braids tested at a strain rate of 2%/s is shown in Fig. 3. In the same figure, a photograph of the ligament construct shows that failure occurred in the intraarticular zone of the scaffold.

3.4. Scaffold in vitro evaluation

The attachment morphology of BALB/C fibroblasts and primary rabbit ACL cells after 24 h of culture are shown in Figs. 4 and 5, respectively. Differences in cell adhesion and spreading on the braided scaffold were observed between both cell types after 1 day of culture. The BALB/C fibroblasts spread readily on the substrate and formed extended cell processes spanning individual fibers of the scaffold. The extension of cell processes was perpendicular to the longitudinal axis of the fibers. The SEM micrographs in Fig. 5 show primary rabbit ACL cells attached unidirectional to the longitudinal axis of the fibers. These cells were largely spherical and exhibited much slower cellular spreading as compared to the BALB/C mouse fibroblast.

Additional differences between the cell types were observed in the longer-term cultures. Cell morphology after 8 days in culture is presented in Figs. 6 (BALB/C) and 7 (rabbit). For both cell types examined, proliferated over the 1-week culturing period. As shown in Fig. 6, extensive cellular growth and the formation of large cellular networks which bridge the fibers were observed for the BALB/C fibroblasts cultured. The growth orientations of these cell sheets were found to be random and the BALB/C mouse fibroblasts response did not correspond to the underlying geometry of the three-dimensional circular braids. In contrast, the primary ACL cells clustered and grew in small groups on the 3-D scaffold. At lower magnification (Fig. 7),

Table 2
Tensile properties of poly-(α-hydroxyester) yarns and scaffolds

Sample ($n = 6$)	Maximum load (N)	Ultimate tensile strength (MPa)
Single multi-filament yarn		
PLAGA (10:90) 52 denier	2.4±.02	5.3±1.8
10-yarn bundle (30 filaments/yarn)		
PLAGA (10:90) 52 denier	25±3	8.8±1.1
PLAGA (10:90) 4 × 12 rectangular braid (9)		
2%/s	606±45	393±29
50%/s	525±28	340±18
100%/s	548±48	439±84
PLAGA (10:90) 3 × 16 Circular Braid (18) 2%/s	907±132	212±25
PLAGA (10:90) 4 × 12 Rectangular Braid (18) 2%/s	705±36	217±11

Note: ( ), the number of yarns per yarn bundle and %/s, strain rate.

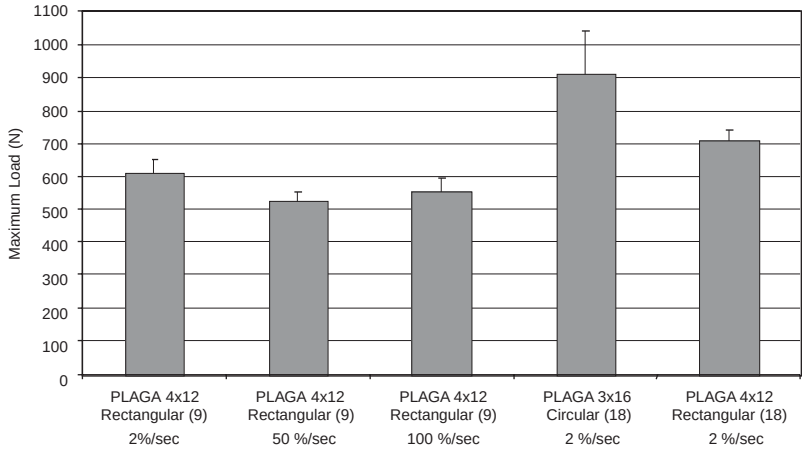

Fig. 2. Maximum load at failure for various 3-D braided scaffolds (in parentheses are the numbers of yarns for particular braid) and strain rate (statistically significant at $p < 0.05$, $n = 6$).

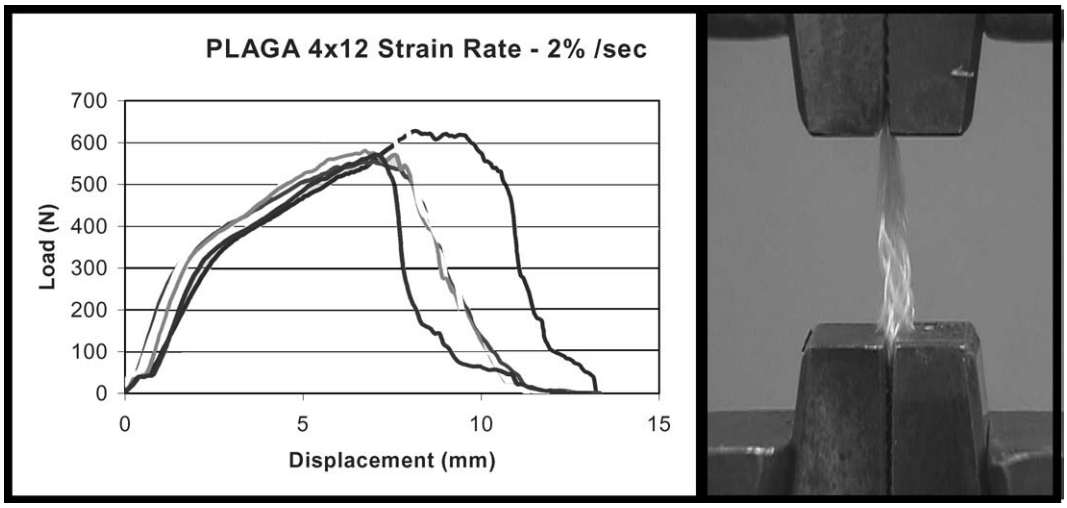

Fig. 3. Load–deformation curve and photomicrograph of mechanical failure of the 4×12 PLAGA 3-D rectangular braids at a strain rate of 2%/s.

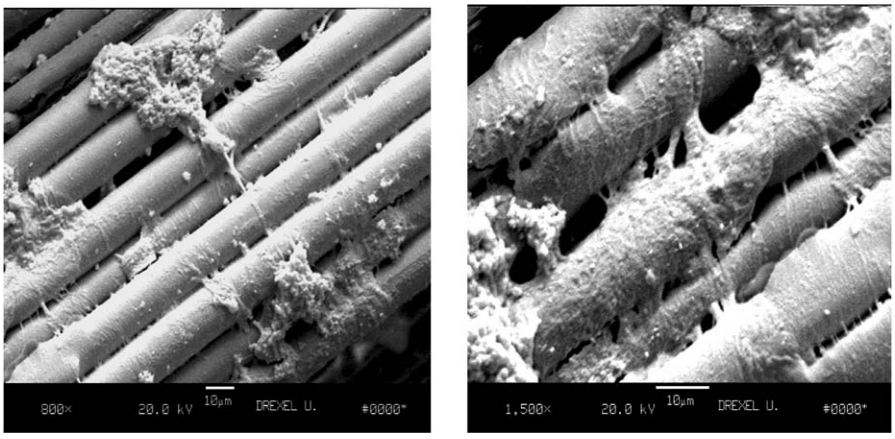

Fig. 4. Electron micrographs of BALB/C mouse fibroblast after 1 day in culture shows cellular spreading across the fiber (left magnification—$800 \times$, 10 μm bar and right magnification—$1500 \times$, 10 μm bar).

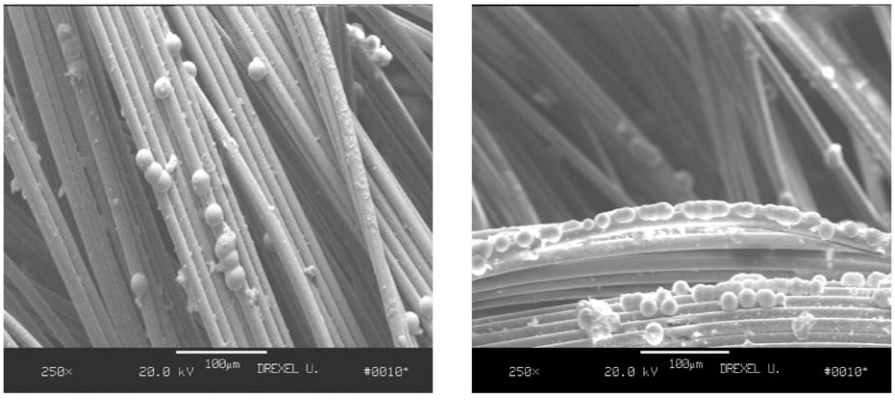

Fig. 5. Electron micrographs of rabbit ACL cells after 1 day in culture shows cell migration and attachment along the fibers (left and right magnification—$250 \times$ and 100 μm bar).

particularly at the intersection between two bundles of the yarn, these cells responded to the underlying geometry and formed confluent areas on the 3-D braided scaffold.

4. Discussion

The primary objective of this study was to develop a novel ACL scaffold for ligament reconstruction,

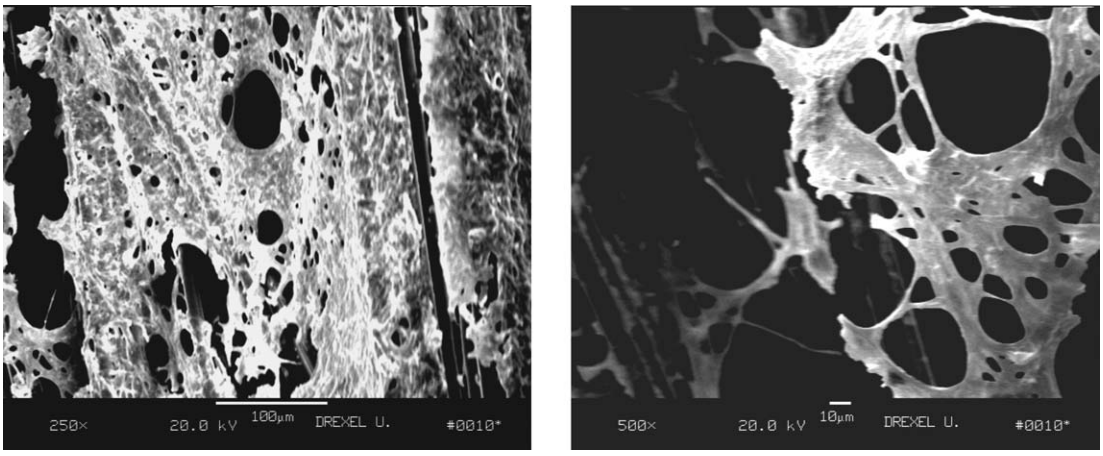

Fig. 6. Electron micrographs of BALB/C mouse fibroblast after 8 days in culture shows large cellular networks with cells proliferating with and without the underlying scaffold (left magnification—250 ×, 100 μm bar and right magnification—500 ×, 10 μm bar).

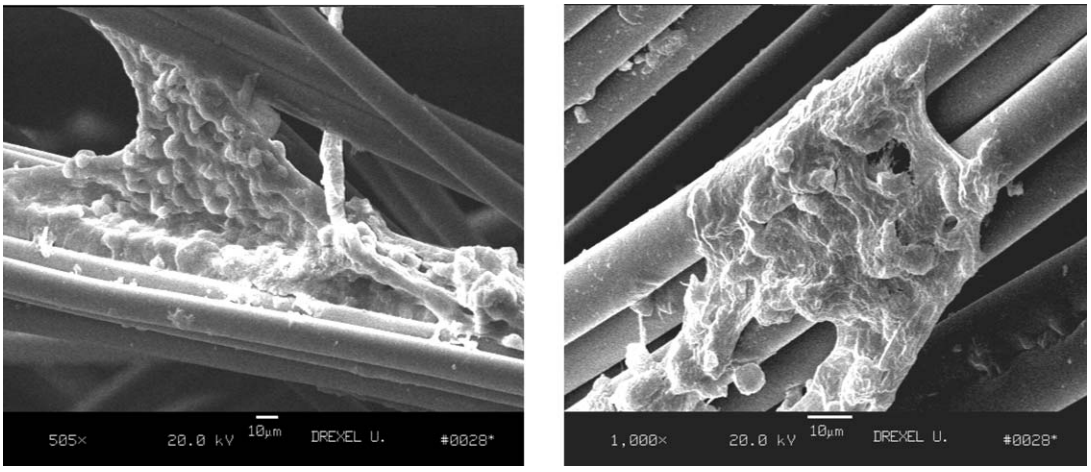

Fig. 7. Electron micrographs of rabbit ACL cells after 8 days in culture shows cell response to 3-D circular braid, the cells did not cover the whole scaffold but did continue to follow the underlying fibrous geometry (left magnification—505 ×, 10 μm bar and right magnification—1000 ×, 10 μm bar).

focusing on scaffold architecture, porosity, degradability, and cell source. Specifically, the novel scaffold was based on a 3-D fibrous hierarchical design, utilizing custom braiding techniques which permits controlled fabrication of substrates with a desired pore diameter, porosity, mechanical properties, and geometry. Such a scaffold would provide the newly regenerating tissue with a temporary site for cell attachment, proliferation, and mechanical stability. As shown in Fig. 1, the 3-D, braided PLAGA fiber scaffold developed was comprised of three regions: femoral bone tunnel attachment site, ligament region, and tibial tunnel attachment site. The attachment sites for the bone tunnels had a lower porosity and smaller pore diameter compared to the ligament region. This pre-designed heterogeneity in the grafts was aimed to promote integration of the graft with bone tissue and resist the abrasive forces within the bone tunnels. The advantages of this system as compared to other systems are controlled porosity and pore diameter to encourage tissue infiltration throughout the scaffold, which are lacking in most ACL artificial implants. The 3-D braiding system allowed for custom production of scaffolds with mechanical properties similar to those of natural ACL tissue in order to overcome issues of stress shielding during tissue ingrowth. In addition, the intertwining of the fibers within the 3-D braid prevents total catastrophic failure of the scaffold due to a small rupture.

Three-dimensional braiding is defined as a system where three or more braiding yarns are used to form an integral braided structure, with a network of continuous filament and yarn bundles with fibrous architecture oriented in various directions. Three-dimensional braiding systems can produce thin and thick structures in a wide variety of shapes through the selection of yarn bundle size [33,34,38,39]. The results of this study demonstrate that processing

parameters such as braiding angle can be manipulated in order to increase or decrease porosity and mode pore diameter. This is critical to the development of tissue-engineered ligaments because there is an optimal pore size that must be created to promote tissue ingrowth. There has been evidence that calcified tissue ingrowth can occur at a lower limit pore size of 100 μm [24,25]. A minimum pore size of 150 μm has been suggested in the literature for bone and 200–250 μm for soft tissue [11,24–26]. Samples that are fabricated with an increasing braiding angle for the same number of carrier yarns, linear density, and scaffold size display increasing total surface area and have smaller pore interconnecting networks or spacing within the scaffold. Therefore, scaffolds with higher braiding angles have decreased porosity and increased total pore surface area due to more material filling the same amount of space when compared to low braiding angle scaffolds of the same size. Based on this rationale, the optimal porosity for the ligament scaffolds should be above 50% to create the optimal pore diameters of 100–300 μm needed for in vivo tissue ingrowth. Consequently, 3-D circular and 3-D rectangular braided scaffolds were fabricated in the optimal pore size range for ligament and bone tissue ingrowth as expressed in the literature [11,24,26].

Previous ligament prostheses have been made of flexible composites consisting of fibers that have been woven or braided into structures [11,14]. These scaffolds performed well for a short period after implantation, while the long-term results have been poor [11,14]. These composite structures were limited by poor tissue integration, poor abrasion resistance, and fatigue failure [11,14]. The 3-D braided structures designed in this study can overcome some of these problems through the development of an interconnected network of porous structures that will help the transportation of oxygen and nutrients throughout the implant site. The flexible, porous 3-D braids allow the regeneration of new tissue between the pores and serve as scaffolds for cell proliferation.

In this study, we compared the structural properties (porosity, elastic modulus, and tensile strength) of two types of braided ligament scaffolds (rectangular and circular), in order to select an optimal braiding geometry for a tissue-engineered ACL scaffold. The results demonstrated that processing parameters such as yarn density, size, and geometry of the scaffold could be optimized with 3-D braiding technology to match initial mechanical properties of living tissue. The designed scaffolds under tension exhibited a very short elastic region with prolonged plastic deformations as strain rates decreased. The ultimate tensile strengths ranged from $\sim$100 to 400 MPa. The maximum load data for the 4×12 rectangular braid showed a significant change with increasing strain rate. The stress–strain profiles looked similar to what would be expected of natural ligament tissue. When the same number of yarns was used for the rectangular and circular braids the circular braid geometry showed a significant increase in maximum tensile load. The 3-D circular fibrous scaffold was able to withstand tensile loads of 907 N (SD $\pm$ 132 N), which was greater than the level for normal human physical activity that is estimated to range between 67 and 700 N [40–42].

In addition to the porosity of the prosthesis, crimp geometry could also be included in the design of the scaffold to mimic the stiffness of natural ligament. The porosity data displayed in Table 1 for both the 3-D circular and rectangular braids show that there must be a significant change in braiding angle to effect change in the total surface area, mode pore diameter, median pore diameter, and porosity. In addition, the data show that yarn bundle size can have a major effect on porosity parameters. The porosity data in Table 1 also demonstrate the capability of a 3-D braiding system to fabricate and control the formation of pore diameters within the 3-D braided scaffold that ranged between 167 and 260 μm, which is conducive for tissue ingrowth. The cellular studies were conducted on the 3-D braided scaffolds with mode pore diameters of 233 μm.

In addition to scaffold architecture and degradability, cell source and cellular response are also important consideration in ACL tissue engineering. In this study, the primary criteria for cell selection was based on whether the alternative cell source could reproduce or mimic the response of native ACL cells when exposed to the designed replacement scaffold.

The results of this study confirm the biocompatibility of the scaffold, as both cell types attached and proliferated on the scaffold. The primary rabbit ACL cells and BALB/C mouse fibroblasts grew on the 3-D biodegradable rectangular braided scaffold. The primary rabbit ACL cells seemed to proliferate and spread at a slower rate compared to the BALB/C fibroblast as observed by the SEM photomicrographs. The 3-D circular braided scaffold design promoted the adhesion and growth of rabbit ACL cells along the longitudinal axis of the fibers. Although the BALB/C mouse fibroblasts created large branched cellular networks on the 3-D circular braids, the cellular organization did not directly respond to scaffold geometry. As a result, BALB/C mouse fibroblasts will not be used in future scaffold studies to measure cell proliferation and viability capacity of the scaffold. In addition, the primary rabbit ACL cells may need to be seeded at a higher density for this scaffold geometry. The addition of biological factors such as growth factors and adhesion proteins to the polymer surface can also enhance the cellular proliferation capabilities of the 3-D braided scaffold.

5. Conclusions

ACL tissue engineering is need because of past failures in ligament reconstruction using prostheses. There has been a rise in the number of ACL reconstructions over the years due to an active population but past replacements have failed because they have not been able to reproduce the biomechanics and function of the normal ACL. In this study, we identified some of the different parameters that must be addressed to produce a biocompatible tissue-engineered ligament replacement. We have devised a method for fabricating a fibrous, biodegradable ligament replacement using 3-D braiding technology. This method produces heterogeneous scaffolds that are able to adapt to the intraarticular region of the ligament, withstand the rigors of surgical fixation within the bone tunnels, and promote guided healing. This study has shown our ability to fabricate a tissue-engineered ligament scaffold that has the mechanical properties of the normal ACL and the porosity for tissue ingrowth. During cell culture, the attachment, spreading, and growth of primary ACL cells and BALB/C mouse fibroblasts demonstrate the biocompatibility of the scaffold. In addition, the oriented growth of the primary rabbit ACL cells suggests the need to use primary cells in ligament tissue engineering.

Future studies will focus on the scaffold's initial mechanical properties as compared to a rabbit model and in vitro characterization of the cellular response and interaction with the braided tissue-engineered ligament scaffold.

Acknowledgements

The National Institutes of Health through grant numbers NIH-AR46117 and NIH-F31GM18905 supported this study. We wish to express our gratitude to Sharron Manuel and Janell Carter for their assistance in the rectangular braid study.

References

[1] Cooper JA, Lu HH, Ko FK, Laurencin CT. Fiber-based tissue engineered scaffold for ligament replacement: design considerations and in vitro evaluation. Mt. Laurel, NJ: Society for Biomaterials; 2000. p. 208.

[2] Cameron ML, Mizung Y, Cosgarea AJ. Diagnosing and managing anterior cruciate ligament injuries. J Musculoskeletal Med 2000;17:47–53.

[3] Friedman MJ, Sherman OH, Fox JM, Pizzo WD, Snyder SJ, Ferkel RJ. Autogenic anterior cruciate ligaments (ACL) anterior reconstruction of the knee. Clin Orthop 1985;196:9–14.

[4] Zavras TD, Mackenney RP, Amis AA. The natural history of anterior cruciate ligament reconstruction using patellar tendon autograft. The Knee 1995;2:211–7.

[5] Jackson DW, Heinrich JT, Simon TM. Biologic and synthetic implants to replace the anterior cruciate ligament. Arthroscopy 1994;10:442–52 [Review] [57 Refs].

[6] Jackson DW, Arnoczky S, Woo SL, Frank CB, Simon TM. The anterior cruciate ligament: current and future concepts. New York: Raven Press; 1993.

[7] Warren RF. Primary repair of the anterior cruciate ligament. Clin Orthop Relat Res 1983;172:65–70.

[8] Arnoczky S, Warren RF, Ashlock MA. Replacement of the anterior cruciate ligament using a patellar tendon allograft. J Bone Jt Surg Am 1986;68A:376.

[9] Hamner DL, Brown CH, Steiner ME, Hecker AT, Hayes WC. Hamstring tendon grafts for reconstruction of the anterior cruciate ligament: biomechanical evaluation of the use of multiple strands and tensioning techniques. J Bone Jt Surg 1999;81A: 549–57.

[10] Laurencin CT, Ambrosio AMA, Borden MD, Cooper JA. Tissue engineering: orthopedic applications. In: Yarmush ML, Diller KR, Toner M, editors. Annual review of biomedical engineering. Palo Alto, CA: Annual Reviews; 1999. p. 19–46.

[11] Yahia L. Ligaments and ligamentoplasties. Berlin, Heidelberg: Springer; 1997.

[12] Paavolainen P, Makisalo S, Skutnabb K, Holmstrom T. Biologic anchorage of cruciate ligament prosthesis: bone ingrowth and fixation of the Gore-Tex ligament in sheep. Acta Orthop Scand 1993;64:323–8.

[13] McPherson GK, Mendenhall HV, Gibbons DF, Plenk H, Rottmann W, Sanford JB, Kennedy JC, Roth JH. Experimental mechanical and histological evaluation of the Kennedy ligament augmentation device. Clin Orthop 1985;196:186–95.

[14] Guidoin MF, Marois Y, Bejui J, Poddevin N, King MW, Guidoin R. Analysis of retrieved polymer fiber based replacements for the ACL. Biomaterials 2000;21:2461–74.

[15] Bercovy M, Goutallier D, Voisin MC, Geiger D, Blanquaert D, Gaudichet A, Patte D. Carbon-PGLA prostheses for ligament reconstruction: experimental basis and short-term results in man. Clin Orthop Relat Res 1985;196:159–68.

[16] Mowbray MAS, McLeod ARM, Barry M, Ciike WD, O'Brien TK. Early failure in an artificial anterior cruciate ligament scaffold. The Knee 1997;4:35–40.

[17] Kock H-J, Sturmer KM, Letsch R, Schmitt-Neuerburg KP. Interface and biocompatibility of polyethylene terepthalate knee ligament prostheses: a histological and ultrastructural device retrieval analysis in failed synthetic implants used for surgical repair of anterior cruciate ligaments. Arch Orthop Trauma Surg 1994;114:1–7.

[18] Laurencin CT, Ko FK, Borden MD, Cooper JA, Li WJ, Attawia M. Fiber based tissue engineered scaffolds for musculoskeletal applications, in vitro cellular response. In: Neenan T, Marcolongo M, Valentini RF, editors. Biomedical materials: drug delivery, implants and tissue engineering: Symposium Held November 30–December 1, 1998. Boston, MA, USA: Materials Research Society, 1999.

[19] Dunn MG, Liesch JB, Tiku ML, Zawadsky JP. Development of fibroblast-seeded ligament analogs for ACL reconstruction. J Biomed Mater Res 1995;29:1363–71.

[20] Jackson DW, Simon TM, Lowery W, Gendler E. Biologic remodeling after anterior cruciate ligament reconstruction using a collagen matrix derived from demineralized bone. An experimental study in the goat model. Am J Sports Med 1996;24: 405–14.

[21] Jackson DW, Simon TM, Lowery W, Gendler E. Biologic remodeling after anterior cruciate ligament reconstruction using a collagen matrix derived from demineralized bone: an experimental study in the goat model. Am J Sports Med 1996;24: 405–14.

[22] Altman GH, Horan RL, Lu HH, Moreau J, Martin I, Richmond JC, Kaplan DL. Silk matrix for tissue-engineered anterior cruciate ligaments. Biomaterials 2002;23:4131–41.
[23] Cooper JA, Sahota J, Gorum J, Carter J, Ko FK, Doty S, Laurencin CT. Evaluation of a novel tissue-engineered ligament: in vivo studies. New Jersey: Society for Biomaterials; Spring 2003 Meeting, p. 162.
[24] Spector M, Michno MJ, Smarook WH, Kwiatkowski GT. A high-modulus polymer for porous orthopedic implants: biomechanical compatibility of porous implants. J Biomed Mater Res 1978;12:665–77.
[25] von Recum AF. Handbook of biomaterials evaluation: scientific, technical and clinical testing of implant materials. New York: Macmillan; 1986.
[26] Konikoff JJ, Billings W, Nelson LJ, Hunter JM. Development of a single stage active tendon prosthesis. I. Distal end attachment. J Bone Jt Surg Am 1974;56:848.
[27] Morgan JR, Yarmush ML. Tissue engineering methods and protocols. New Jersey: Humana Press Inc.; 1999.
[28] Wise DL, Trantolo DJ, Altobelli DE, Yaszemski MJ, Gresser JD, Schwartz ER. Encyclopedic handbook of biomaterials and bioengineering—Part A: materials. New York, NY: Marcel Dekker; 1995.
[29] Wise DL, Trantolo DJ, Altobelli DE, Yaszemski MJ, Gresser JD, Schwartz ER. Encyclopedic handbook of biomaterials and bioengineering—Part B: applications. New York, NY: Marcel Dekker; 1995.
[30] Nigg BM, Herzog W. Biomechanics of the musculo-skeletal system. New York: Wiley; 1994.
[31] Frank CB, Woo SL, Andriacchi T, et al. Injury and repair of the musculoskeletal soft tissues. Park Ridge, IL: American Academy of Orthopedic Surgeons; 1988. p. 45–101.
[32] Laurencin C, Attawia M, Botchwey E, Warren R, Attia E. Cell-material systems for anterior cruciate ligament regeneration. In Vitro Cell Dev Biol Anim 1998;34:90–2 [letter].
[33] Ko FK, Pastore CM, Head AA. Handbook of industrial braiding. Covington, KY: Atkins and Pearce, Inc.; 1989.
[34] Ko FK. Braiding. Engineering materials handbook: composites, vol. 1. Metals Park, OH: ASM International; 1987. p. 519–28.
[35] Ko FK. Three-dimensional fabrics for composites. In: Chou TW, Ko FK, editors. Textile structural composites. Amsterdam: Elsevier; 1989. p. 129–71.
[36] Amiel D, Nagineni CN, Choi SH, Lee J. Intrinsic properties of ACL and MCL cells and their responses to growth factors. Med Sci Sports Exercise 1995;27:844–51.
[37] Botchwey EA, Pollack SR, Levine EM, Laurencin CT. Bone tissue engineering in a rotating bioreactor using a microcarrier matrix system. J Biomed Mater Res 2001;55(2):242–53.
[38] Ko FK, Soebroto HB, Lei C. 3-D net shaped composites by the 2-step braiding process. SAMPE J 1988;33:912–32.
[39] Ko FK, Pastore CM. Structure and properties of an integrated 3-D fabric for structural composites. Am Soc Test Mater STP 1985;864:428–39.
[40] Chen EH, Black J. Materials design analysis of the prosthetic anterior cruciate ligament. J Biomed Mater Res 1980;14:567–86.
[41] Black J. Biological performance of materials: fundamentals of biocompatibility, 2nd ed.. New York: Marcel Dekker; 1992.
[42] Black J, Hastings G. Handbook of biomaterial properties, 1st ed. London, UK: Chapman & Hall; 1998.